AIP | Applied Physics Letters

Temperature dependence of Brillouin light scattering spectra of acoustic phonons in silicon

Kevin S. Olsson, Nikita Klimovich, Kyongmo An, Sean Sullivan, Annie Weathers, Li Shi, and Xiaoqin Li

Citation: Applied Physics Letters **106**, 051906 (2015); doi: 10.1063/1.4907616
View online: http://dx.doi.org/10.1063/1.4907616
View Table of Contents: http://scitation.aip.org/content/aip/journal/apl/106/5?ver=pdfcov
Published by the AIP Publishing

Temperature dependence of Brillouin light scattering spectra of acoustic phonons in silicon

Kevin S. Olsson,[1] Nikita Klimovich,[1] Kyongmo An,[1] Sean Sullivan,[2,3] Annie Weathers,[4] Li Shi,[3,4,a)] and Xiaoqin Li[1,3,a)]
[1]*Department of Physics, Center of Complex Quantum Systems, The University of Texas at Austin, Austin, Texas 78712, USA*
[2]*Materials Science and Engineering Program, The University of Texas at Austin, Austin, Texas 78712, USA*
[3]*Texas Materials Institute, The University of Texas at Austin, Austin, Texas 78712, USA*
[4]*Department of Mechanical Engineering, The University of Texas at Austin, Austin, Texas 78712, USA*

(Received 3 November 2014; accepted 24 January 2015; published online 6 February 2015)

Electrons, optical phonons, and acoustic phonons are often driven out of local equilibrium in electronic devices or during laser-material interaction processes. The need for a better understanding of such non-equilibrium transport processes has motivated the development of Raman spectroscopy as a local temperature sensor of optical phonons and intermediate frequency acoustic phonons, whereas Brillouin light scattering (BLS) has recently been explored as a temperature sensor of low-frequency acoustic phonons. Here, we report the measured BLS spectra of silicon at different temperatures. The origins of the observed temperature dependence of the BLS peak position, linewidth, and intensity are examined in order to evaluate their potential use as temperature sensors for acoustic phonons. © *2015 AIP Publishing LLC*. [http://dx.doi.org/10.1063/1.4907616]

Thermal management represents an outstanding challenge in many areas of technology. In microelectronics based on silicon, local hot spots have become a significant barrier for further miniaturization of devices according to the Moore's law. In high-field electronic devices, as well as laser-material interaction processes, hot electrons are often coupled more strongly to optical phonons than to acoustic phonons, the dominant heat carriers in silicon and other semiconductors.[1–3] In addition, the relatively slow decay process of optical phonons to acoustic phonons leads to a phonon bottleneck in the energy dissipation processes according to a number of theoretical studies.[4–7] However, there have been few direct experimental observations of such highly non-equilibrium transport processes.[8,9] Direct measurements are needed for better understanding the coupling and non-equilibrium transport processes of different energy carriers in semiconductors and for designing next-generation electronic devices to overcome the thermal management challenge.

This need has driven the active development of both scanning probe microscopy and optical microscopy techniques for probing the local temperatures of different energy carriers in operating electronic devices.[8–16] Compared to thermal reflectance and scanning probe based thermometry methods, inelastic light scattering based techniques can potentially achieve high spectral resolution for specific phonon modes.[17,18] Raman scattering is a widely used inelastic scattering method, employed to probe phonon transport in various materials.[8–16,19,20] One limitation, however, is that Raman scattering mainly probes high-frequency optical phonon modes. Consequently, the peak intensity can be used to probe only the population and equivalent temperature of such optical phonons. In addition, the population or temperature of intermediate frequency phonons can play an important role in the observed temperature dependence of the peak position and linewidth of the Raman-active optical phonons.[21–24] Existing Raman thermometry techniques are not capable of spectrally resolving the equivalent temperature of low-frequency acoustic phonons. Recent time domain and frequency domain thermal reflectance measurements have indirectly revealed the presence of ballistic low-frequency phonons for thermal length scales smaller than the phonon mean free path.[25–27] These ballistic, long mean free path phonons are likely not at local equilibrium with intermediate and high frequency phonons in nanostructures and microelectronic devices.[28–30] However, measurements have not been able to directly probe the local non-equilibrium temperatures of different phonon modes. Therefore, there is currently a lack of methods for measuring the low-frequency acoustic phonon temperature.

Brillouin light scattering is an inelastic light scattering technique whose principle is identical to Raman scattering but is used much less frequently due to technical challenges. One major difference is the use of a specialized tandem-multipass interferometer based on scanning Fabry-Perot cavities to resolve scattered light with small frequency shifts ($<$200 GHz).[31] While acoustic phonons have been probed using stimulated Brillouin spectroscopy and picosecond ultrasonic techniques, such techniques are based on the optical excitation of a large population of acoustic phonons, which is undesirable in thermometry measurements.[32,33] Recently, Brillouin light scattering (BLS) techniques have been used as a local temperature sensor for magnons in metallic and insulating ferromagnetic materials and for low-frequency phonons in glass.[34,35] However, the application of this thermometry method for acoustic phonons in semiconductors remains to be investigated.

In this paper, we report an investigation of the temperature dependence of the BLS spectra of silicon, the most common electronic material. For comparison, Raman measurements are

a)Authors to whom correspondence should be addressed. Electronic addresses: lishi@mail.utexas.edu and elaineli@physics.utexas.edu

taken simultaneously with the BLS measurements. Both BLS and Raman spectra of uniformly heated silicon exhibit systematic changes in frequency shift, linewidth, and the integrated intensity. In particular, the apparent BLS spectra exhibit an upward frequency shift with increasing temperature, opposite to that of the Raman spectra. This observation is explained by considering the sensitive dependence of the BLS frequency on wave vector, and thus, the refractive index of the material. Better understanding of the origins of the observed temperature dependence of the BLS spectra may allow the establishment of BLS as a thermometry technique for low-frequency acoustic phonons in semiconductors.

Our experimental setup is shown in Fig. 1(a). A (110) Si sample was mounted on a ceramic heater. A single frequency 532 nm, p-polarized laser, incident at 45° from the surface normal (angle not depicted in Fig. 1(a)), was used to probe the phonon modes. The [001] axis of the Si was aligned along the p direction. The scattered light was collected in backscattering geometry, where a beam splitter directed approximately 4% of the scattered light to a spectrometer and a Si charge coupled detector (CCD) for Raman measurements. The rest of the collected scattered light was directed to a Tandem Multipass Fabry-Perot interferometer for BLS measurements. A representative BLS spectrum, shown in Fig. 1(b), shows two peaks, corresponding to the longitudinal acoustic (LA) phonon along the [110] direction and the transverse acoustic (TA) phonon modes along the [001] direction. The phonon frequency measured in the BLS spectra is given by

$$2\pi f = 2nvk_0, \tag{1}$$

where n is the index of refraction of silicon, v is the group velocity of the phonon mode, and k_0 is the wave vector of the incident light.[36] The phonon modes we observed agree with the frequencies predicted using an incident wave vector of $1.18 \times 10^7\ \mathrm{m}^{-1}$ and group velocities of 5.834×10^3 m/s and 9.167×10^3 m/s, for the TA and LA phonons, respectively.[37] In our temperature analysis of the BLS spectra, we choose to focus on the LA phonon mode over the TA mode because of its relatively high signal to noise ratio. In the Raman spectra, shown in Fig. 1(c), we observed one phonon peak corresponding to the degenerate optical modes near the Brillouin zone center.[38]

Next, the sample was uniformly heated, in 30 K increments, from 298 K to 568 K, and probed with an incident laser power of 150 mW. The temperature was measured by a thermocouple attached to the heater close to the sample. At each temperature, the sample was allowed to equilibrate for 10 min before BLS and Raman spectra were measured for a total of 45 min and 38 min, respectively. We fit the phonon peaks with Lorentzian lineshapes at each temperature, shown in Fig. 2. There is a clear downward shift in frequency for the Raman spectra as temperature increases. This frequency shift is due to bond softening and the increased scattering with intermediate frequency phonons at higher temperatures as suggested in previous studies.[22,23,39] The BLS spectra, shown in Fig. 2, have an apparent upward shift in frequency as temperature increases, opposite to the downward shift predicted by the decreasing phonon group velocity.[37] The phonon frequency shifts are explicitly plotted as a function of temperature by extracting the centers from the Lorentzian fits. The temperature dependent BLS and Raman frequency both fit to linear functions quite well in the temperature range examined, as shown in Fig. 3(a). We note that the probing laser may cause local heating. However, since the probing laser power remains the same for the temperature calibration process and for local temperature sensing, the

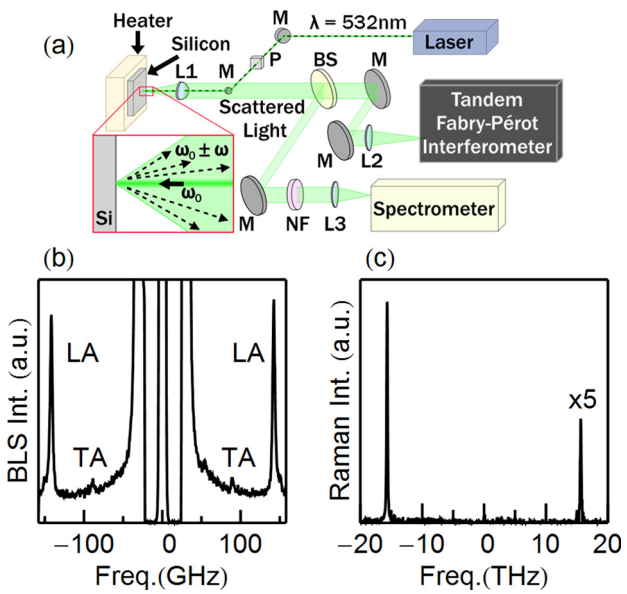

FIG. 1. (a) Schematic diagram of experimental set-up. Key components include a 532 nm laser, mirrors (M), a polarizer (P), several lenses (L1,L2,L3), a beam splitter (BS), a 532 nm notch filter (NF), a spectrometer for Raman measurements, and a tandem Fabry-Perot interferometer for BLS measurements. (b) A representative BLS spectrum of Si measured for 120 min, with incident laser power 150 mW at room temperature. LA and TA represent the longitudinal and transverse acoustic phonon modes, respectively. (c) An example Raman spectrum, measured for 38 min at 150 mW incident laser power at room temperature.

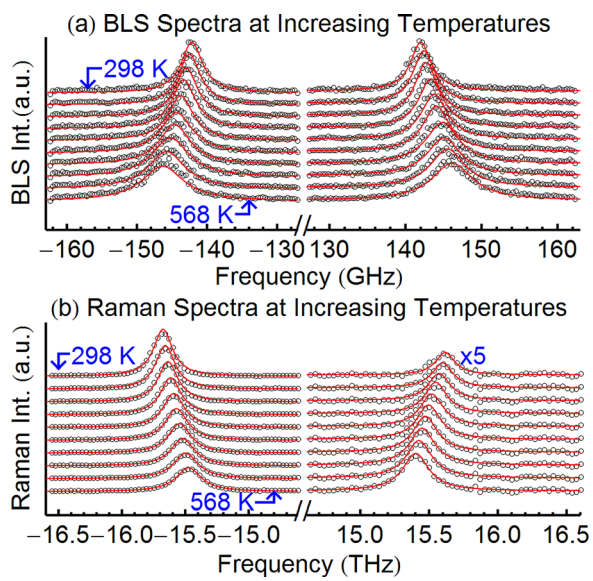

FIG. 2. (a) BLS and (b) Raman spectra are plotted for each temperature (black circles) along with the Lorentzian fits (red lines). The top most curves on each plot correspond to the measurements made at 298 K, with the temperature increasing in increments of 30 K as the curves move toward the bottom of the charts, ending with the plot corresponding to the measurement at 568 K.

effect does not compromise the accuracy of our method for measuring temperature rise caused by other heating sources.

The apparent opposite temperature dependence shown by the acoustic phonon frequency can be understood by taking into account the temperature dependence of the refractive index of Si, which influences the probed phonon frequency according to Eq. (1). By conducting ellipsometry measurements as a function of temperature, we directly extracted the temperature-dependent refractive index. A downward frequency shift in the BLS frequency is obtained, shown in Fig. 3(b), after removing the effect of temperature dependent refractive index, shown in Fig. 3(c). Such a downward shift in the acoustic phonon frequency is related to the decreased group velocity, caused by bond softening.

The BLS linewidth is also found to increase with increasing temperature, as shown in Fig. 4(a). First principle methods have been used to calculate anharmonic linewidths in graphene, silicon, and germanium.[24,40–43] It has been suggested that the decay of one phonon into two lower frequency phonons, and the combination of two phonons into a higher frequency phonon scattering processes both contribute to the anharmonic linewidth for the LA phonon modes of silicon.[24] Further studies are required to investigate whether the temperature dependence of the anharmonic phonon linewidth or another mechanism has led to the observed temperature dependence of the BLS linewidth.

We further investigate the integrated intensity of the BLS peaks as a possible method for measuring the population or equivalent temperature of the low-frequency acoustic phonons that yield the BLS peaks. The intensity of the BLS signal is given by

$$I = \frac{\varepsilon^4 \hbar V {\omega_s}^4 \omega_p}{2{\varepsilon_0}^4 (4\pi)^2 c^4 \varrho \upsilon^2} |\hat{e}_s \cdot \vec{P} \cdot \hat{e}_i|^2 \left\{ \begin{matrix} n+1 \\ n \end{matrix} \right\} I_0, \qquad (2)$$

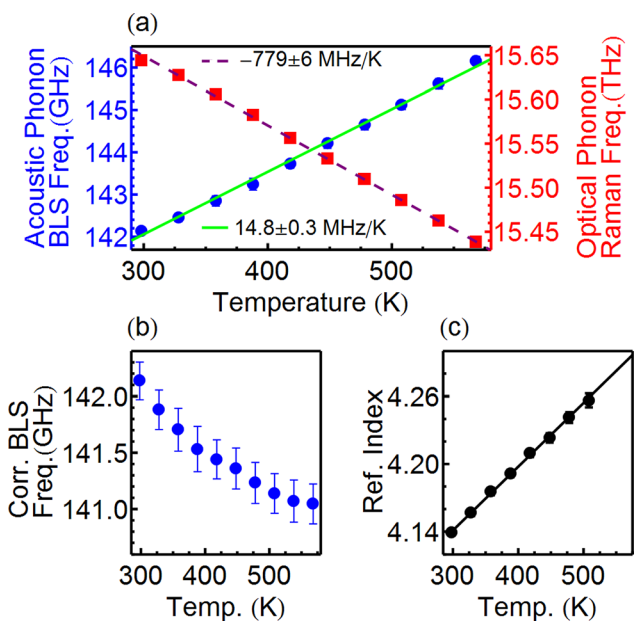

FIG. 3. (a) Directly measured acoustic and optical phonon frequency shift as a function of temperature extracted from the BLS (circles, left axis) and Raman (squares, right axis) spectra. (b) Corrected acoustic phonon frequency decreases with temperature. (c) Ellipsometry measurements show that the refractive index increases with temperature.

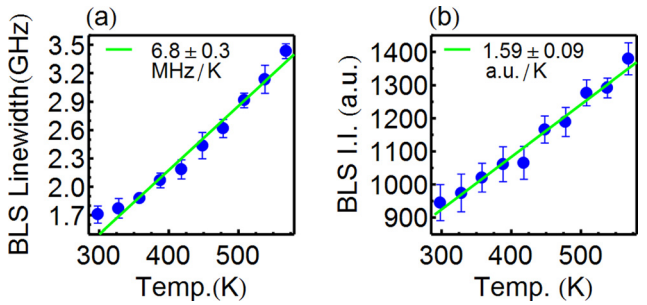

FIG. 4. (a) Linewidths of the acoustic phonon measured from the full width half maxima of the Lorentzian fits to the BLS spectra. (b) The integrated intensity (I.I.) for the BLS Stokes peak increases approximately linearly with temperature. The refractive index effect has not been removed.

where ε is the permittivity of silicon, ε_0 is the permittivity of free space, $\hbar$ is the reduced Planck constant, V is the scattering volume, ω_s is the scattered frequency, ω_p is the frequency of the phonon, c is the speed of light in vacuum, ϱ is the density, υ is the group velocity of the phonon, $\hat{e}_s$ ($\hat{e}_i$) is the polarization of the scattered (incident) light, $\vec{P}$ is the photoelastic tensor contracted with the unit vectors of the phonon propagation and phonon polarization, n is the phonon occupation given by the Bose-Einstein distribution, $n+1$ or n corresponds to Stokes or anti-Stokes scattering, and I_0 is the incident intensity.[44] The most significant factor in the temperature dependence of the BLS intensity is the phonon occupation, which increases by approximately 100% over the temperature range between 298 and 568 K. The other temperature dependent quantities can be evaluated via their relation to the permittivity. The photoelastic tensor is approximately proportional to the inverse of the permittivity, leading the BLS intensity to be proportional to the square of the permittivity.[44–46] The scattering volume is determined by the laser spot size, which is independent of temperature, and the penetration depth of the light, which is proportional to the inverse of the imaginary part of the index of refraction through the Beer-Lambert law.[47] The complex refractive index (or equivalently the permittivity) as a function of temperature was measured using ellipsometry. The permittivity was found to increase by approximately 12% over the temperature range, and the imaginary part of the index of refraction showed no clear trend within the 20% uncertainty of the measurements. The changes in the other factors in the BLS intensity are about 3% or less and therefore negligible. In Fig. 4(b), the BLS integrated intensity, dominated by the phonon population change, is shown to linearly increase with temperature. A linear change is expected for low frequency phonons based on the Bose-Einstein distribution, $n = (\exp[\hbar\omega_p/k_B T] - 1)^{-1} \cong k_B T/\hbar\omega_p$, where k_B is Boltzmann's constant, and T is the temperature of the acoustic phonon. As the sample temperature is raised uniformly by the external heater, we assume that the acoustic phonons are thermalized, and their temperature is equivalent to the temperature of the heater. The integrated intensity of the anti-Stokes peak shows a similar linear dependence on temperature (data not shown). In principle, one can establish a one-to-one correspondence between the modified integrated BLS intensity and the population or temperature of the BLS-active acoustic

phonon mode once the effects of other temperature dependent quantities are accounted for via independent ellipsometry measurements.

The intensity ratio between the Stoke and anti-Stoke peaks in BLS does not vary with temperature, in contrast to Raman spectra. This difference arises from the phonon occupancy number for acoustic and optical phonons. Based on the Bose-Einstein distribution $n = (\exp[\hbar\omega_p/k_B T] - 1)^{-1}$, the occupancy number n for the acoustic phonons at 150 GHz is about 41 at room temperature. As a result, the $(n+1)/n$ ratio or the BLS Stokes-to-anti-Stokes ratio is close to 1 and insensitive to temperature. In comparison, the occupancy number is as small as 0.1 for 15 THz optical phonons at room temperature, so that the Raman Stokes-to-anti-Stokes ratio sensitively depends on temperature.

We highlight a number of differences in the temperature dependences of the BLS and Raman spectra. First, the coupling strength of light to optical phonon modes is significantly higher than that to the acoustic phonon modes, because of the larger polarization associated with optical phonons out-of-phase atomic motion within a unit cell.[48] In addition, multiple passes through the scanning Fabry-Perot cavities used by BLS reduce transmission, leading to a loss of signal. Thus, the BLS measurement is significantly more time-consuming because of the low intensity of the scattered photons reaching the detector. In order to collect sufficient scattered photons in a reasonable amount of time, a large optical power is required, which may cause local heating and a constant temperature shift in the probed region. Second, BLS is more sensitive to refractive index changes because the acoustic phonons follow a positive, linear dispersion curve and the optical phonons follow a relatively flat dispersion curve in the low wave vector range probed by light scattering techniques.[38] The increase in the refractive index changes the wave vector in silicon, causing an increase in the measured frequency of the acoustic phonons and little change in the measured optical phonon frequency. Third, because of the low frequency range probed by the BLS measurements, one cannot rely on the anti-Stokes and Stokes ratio as a method for temperature calibration.

We now discuss the accuracy of BLS based temperature sensors. If one relies on the integrated intensity as the temperature sensor, fluctuations in the signal intensity are the limiting factor. The main source of random noise is the slight misalignment of the scanning cavities in the BLS interferometer and is reduced by taking longer integration time in the measurements. For the measurements reported in Fig. 4(b), the average uncertainty in the BLS intensity temperature sensor is approximately 30 K. If one relies on the frequency shift or the linewidth as an empirical temperature sensor instead, the minimal measurable temperature changes are dependent on the frequency resolution of the instrument as well as the signal to noise ratio of the spectra. For the purpose of temperature sensing, the correction in the wave vector is not necessary. Based on the data presented in Fig. 3(a), the uncertainty in frequency-shift based temperature sensing is about 10 K, which is more accurate than the integrated BLS intensity-based temperature sensor. Finally, the BLS linewidth provides a temperature sensitivity of about 20 K based on Fig. 4(a).

It is important to clarify the nature of the temperatures measured by the different BLS parameters. The temperature measured by the empirical frequency shift is not simply determined by the occupation number of the specific BLS probed mode. The measured temperature is affected by a range of phonons, coupled to the probed mode via the anharmonic terms in the interatomic potential, affecting the frequency of the probed phonon mode through the refractive index and the group velocity.[37,49] Similarly, anharmonic phonon interactions and possibly other factors determine the linewidth of the probed phonon mode. Consequently, the frequency and linewidth can be used as empirical temperature sensors, but this measured temperature represents the average temperature of a range of different phonon modes. However, the integrated BLS intensity is proportional to the phonon occupation number for a specific mode, allowing the integrated BLS intensity to be used as a phonon-mode specific temperature sensor. As the relative uncertainty is lower in both the frequency shift and linewidth, these parameters can be used to measure phonon temperature in systems with local equilibrium. However, if one is interested in the temperature of a particular phonon mode in a highly non-equilibrium system in which different phonon modes may have different temperatures, one needs to use to the integrated BLS intensity with the compromise of increased uncertainty.

In summary, we report the temperature dependence in the peak position, linewidth, and intensity of the BLS spectra in Si and discuss qualitatively the origins of these changes. We suggest that these temperature dependent quantities can be used as local temperature sensors although only the integrated intensity is proportional to the occupancy of the specific phonon mode probed. The temperature sensitivity can improve with longer measurement times. In conjunction with the established application of Raman scattering technique as a probe for optical phonons, BLS, sensitive to low frequency acoustic phonon modes, may enable investigations of non-equilibrium transport and coupling of different phonon modes in silicon and other novel nanoelectronic devices.

This work was supported by National Science Foundation (NSF) Thermal Transport Processes Program under Grant No. CBET-1336968.

[1]K. Fushinobu, A. Majumdar, and K. Hijikata, J. Heat Transfer **117**, 25 (1995).
[2]J. Lai and A. Majumdar, J. Appl. Phys. **79**, 7353 (1996).
[3]K. Raleva, D. Vasileska, S. M. Goodnick, and M. Nedjalkov, IEEE Trans. Electron Devices **55**, 1306 (2008).
[4]C. L. Tien, A. Majumdar, and F. M. Gerner, *Microscale Energy Transport* (Taylor & Francis, Washington, D.C., 1998).
[5]E. Pop, S. Sinha, and K. E. Goodson, Proc. IEEE **94**, 1587 (2006).
[6]S. Sinha, E. Pop, R. W. Dutton, and K. E. Goodson, J. Heat Transfer **128**, 638 (2006).
[7]C. J. Ni, Z. Aksamija, J. Y. Murthy, and U. Ravaioli, J. Comput. Electron. **11**, 93 (2012).
[8]S. Berciaud, M. Y. Han, K. F. Mak, L. E. Brus, P. Kim, and T. F. Heinz, Phys. Rev. Lett. **104**, 227401 (2010).
[9]D. H. Chae, B. Krauss, K. von Klitzing, and J. H. Smet, Nano Lett. **10**, 466 (2010).
[10]R. Ostermeir, K. Brunner, G. Abstreiter, and W. Weber, IEEE Trans. Electron Devices **39**, 858 (1992).
[11]I. Calizo, F. Miao, W. Bao, C. N. Lau, and A. A. Balandin, Appl. Phys. Lett. **91**, 071913 (2007).

[12]W. W. Cai, A. L. Moore, Y. W. Zhu, X. S. Li, S. S. Chen, L. Shi, and R. S. Ruoff, Nano Lett. **10**, 1645 (2010).
[13]C. Faugeras, B. Faugeras, M. Orlita, M. Potemski, R. R. Nair, and A. K. Geim, ACS Nano **4**, 1889 (2010).
[14]M. Freitag, H. Y. Chiu, M. Steiner, V. Perebeinos, and P. Avouris, Nat. Nanotechnol. **5**, 497 (2010).
[15]I. Jo, I. K. Hsu, Y. J. Lee, M. M. Sadeghi, S. Kim, S. Cronin, E. Tutuc, S. K. Banerjee, Z. Yao, and L. Shi, Nano Lett. **11**, 85 (2011).
[16]A. A. Balandin, Nat. Mater. **10**, 569 (2011).
[17]S. Huxtable, D. G. Cahill, V. Fauconnier, J. O. White, and J. C. Zhao, Nat. Mater. **3**, 298 (2004).
[18]A. Majumdar, Annu. Rev. Mater. Sci. **29**, 505 (1999).
[19]T. R. Hart, R. L. Aggarwal, and B. Lax, Phys. Rev. B **1**, 638 (1970).
[20]A. Sarua, A. Bullen, M. Haynes, and M. Kuball, IEEE Trans. Electron Devices **54**, 1838 (2007).
[21]R. A. Cowley, Rep. Prog. Phys. **31**, 123 (1968).
[22]M. Balkanski, R. F. Wallis, and E. Haro, Phys. Rev. B **28**, 1928 (1983).
[23]J. Menendez and M. Cardona, Phys. Rev. B **29**, 2051 (1984).
[24]G. Deinzer, G. Birner, and D. Strauch, Phys. Rev. B **67**, 144304 (2003).
[25]Y. K. Koh and D. G. Cahill, Phys. Rev. B **76**, 075207 (2007).
[26]A. J. Minnich, J. A. Johnson, A. J. Schmidt, K. Esfarjani, M. S. Dresselhaus, K. A. Nelson, and G. Chen, Phys. Rev. Lett. **107**, 095901 (2011).
[27]K. T. Regner, D. P. Sellan, Z. H. Su, C. H. Amon, A. J. H. McGaughey, and J. A. Malen, Nat. Commun. **4**, 1640 (2013).
[28]G. Chen, J. Heat Transfer **118**, 539 (1996).
[29]N. Mingo and D. A. Broido, Nano Lett. **5**, 1221 (2005).
[30]G. D. Mahan and F. Claro, Phys. Rev. B **38**, 1963 (1988).
[31]S. M. Lindsay, M. W. Anderson, and J. R. Sandercock, Rev. Sci. Instrum. **52**, 1478 (1981).
[32]P. Dainese, P. S. J. Russell, N. Joly, J. C. Knight, G. S. Wiederhecker, H. L. Fragnito, V. Laude, and A. Khelif, Nat. Phys. **2**, 388 (2006).
[33]B. C. Daly, T. B. Norris, J. Chen, and J. B. Khurgin, Phys. Rev. B **70**, 214307 (2004).
[34]M. Agrawal, V. I. Vasyuchka, A. A. Serga, A. D. Karenowska, G. A. Melkov, and B. Hillebrands, Phys. Rev. Lett. **111**, 107204 (2013).
[35]D. R. Birt, K. An, A. Weathers, L. Shi, M. Tsoi, and X. Q. Li, Appl. Phys. Lett. **102**, 082401 (2013).
[36]J. R. Sandercock, Phys. Rev. Lett. **28**, 237 (1972).
[37]H. J. McSkimin, J. Appl. Phys. **24**, 988 (1953).
[38]S. Q. Wei and M. Y. Chou, Phys. Rev. B **50**, 2221 (1994).
[39]H. Tang and I. P. Herman, Phys. Rev. B **43**, 2299 (1991).
[40]N. Bonini, J. Garg, and N. Marzari, Nano Lett. **12**, 2673 (2012).
[41]D. A. Broido, M. Malorny, G. Birner, N. Mingo, and D. A. Stewart, Appl. Phys. Lett. **91**, 231922 (2007).
[42]N. Bonini, M. Lazzeri, N. Marzari, and F. Mauri, Phys. Rev. Lett. **99**, 176802 (2007).
[43]A. Debernardi, S. Baroni, and E. Molinari, Phys. Rev. Lett. **75**, 1819 (1995).
[44]M. Cardona and G. Güntherodt, Top. Appl. Phys. **50**, 19 (1982).
[45]D. K. Biegelsen, Phys. Rev. Lett. **32**, 1196 (1974).
[46]M. Cardona and G. Güntherodt, *Light Scattering in Solids* (Springer-Verlag, Berlin, New York, 1975).
[47]H. Kuzmany, *Solid-State Spectroscopy: An Introduction* (Springer Verlag, Berlin; New York, 1998).
[48]C. Kittel, *Introduction to Solid State Physics*, 7th ed. (Wiley, New York, 1996).
[49]P. Lautenschlager, M. Garriga, L. Vina, and M. Cardona, Phys. Rev. B **36**, 4821 (1987).